Toward a Terawatt-Scale Sub-10-fs Laser Technology

M. Nisoli, S. Stagira, S. De Silvestri, O. Svelto, S. Sartania, Z. Cheng, Gabriel Tempea, Christian Spielmann, and Ferenc Krausz, *Member, IEEE*

(Invited Paper)

***Abstract*— Powerful techniques for spectral broadening and ultrabroad-band dispersion control, which allow compression of high-energy femtosecond pulses to a duration of a few optical cycles, are analyzed. Spectral broadening in a gas-filled hollow fiber and compression by chirped mirrors with high-energy 20-fs input pulses are presented. Using 1-mJ seed pulses we have demonstrated the generation of 0.5-mJ 5-fs pulses at 0.8-μm and 1-kHz repetition rate. General design criteria to scale the compression technique toward the terawatt level are presented.**

***Index Terms*—Femtosecond laser, pulse compression.**

I. Introduction

FEMTOSECOND laser pulses are essential to the investigation of many important processes in physics, chemistry, biology and electronics. A significant step forward in the generation of femtosecond pulses was made in 1981 with the development of the colliding pulse mode-locked (CPM) dye laser [1], with the first demonstration of sub-100-fs laser pulses. Pulses as short as 27 fs were generated in 1984 using a prism-controlled CPM laser [2]. The evolution of the femtosecond dye laser technology during the 1980's has revolutionized molecular and condensed-matter spectroscopy. An extremely important break-through in the technology of femtosecond lasers was achieved in 1991 with the first demonstration of the self-mode-locked Ti:sapphire laser by Sibbett *et al.* [3]. This achievement triggered a renaissance of solid state lasers. Since then, a dramatic reduction in achievable pulse duration was obtained. Pulses as short as 7.5 fs have been directly generated by a Kerr-lens mode-locked Ti:sapphire oscillator by using chirped mirrors for intracavity dispersion control [4] and, more recently, self-starting 6.5-fs pulses were generated by using prism pairs in combination with a double-chirped mirror and a broad-band semiconductor saturable absorber mirror [5]. In parallel with this progress in femtosecond pulse generation, the introduction of the technique of chirped-pulse amplification (CPA) [6] has made possible the amplification of ultrashort pulses to unprecedented power levels. Pulses as short as 20 fs have now become available with terawatt peak powers at repetition rates of 10–50 Hz [7]–[9] and with multigigawatt peak power at kilohertz rates [10]–[11].

Ultrashort pulses can also be generated by extracavity compression techniques. In 1981 Nakatsuka *et al.* [12] introduced a method for optical pulse compression based on the interplay between self-phase modulation (SPM) and group velocity dispersion (GVD) that arise during the propagation of short light pulses in single-mode optical fibers. The propagation of the pulse along the optical fiber spectrally broadens and chirps the laser pulse as a result of the combined action of SPM and GVD. The spectrally broadened pulse is subsequently compressed in a carefully designed optical dispersive delay line. The increased spectral bandwidth of the output pulse enables to generate a compressed pulse shorter in duration than the input pulse. Using this technique pulses as short as 6 fs at 620 nm were obtained in 1987 from 50-fs pulses generated by a CPM dye laser [13]. More recently, 13-fs pulses from a cavity-dumped Ti:sapphire laser were compressed to 4.6 fs with the same technique using a prism chirped mirror Gires–Tournois interferometer compressor [14], [15]. However, the use of single-mode optical fibers limits the pulse energy to a few nanojoules. In 1996, a powerful pulse compression technique based on spectral broadening in a hollow fiber filled with noble gases has demonstrated the capability of handling high-energy pulses (submillijoule range) [16]. This technique presents the advantages of a guiding element with a large diameter mode and of a fast nonlinear medium with high damage threshold (tunnel ionization). The implementation of the hollow-fiber technique using 20-fs seed pulses from a Ti:sapphire system [10] and a high-throughput broadband prism chirped-mirror dispersive delay line has led to the generation of multigigawatt 4.5-fs pulses with an energy of 20 μJ [17], [18]. A prerequisite for achieving this result was the realization of a negative group delay dispersion (GDD) nearly constant over the wavelength range of 650–950 nm in the delay stage. This performance relied on the use of prisms (in addition to chirped mirrors), limiting the extractable pulse energy to a few tens of microjoules because of the onset of nonlinearities in the prisms at higher pulse energies. More recently, advances in the design of chirped multilayer coatings led to the demonstration of chirped mirrors providing adequate

Manuscript received October 31, 1997.. This work was supported by the CNR, by the Istituto Nazionale per la Fisica della Materia, Italy, and by the FWF and the Ministry of Science and Arts in Austria.

M. Nisoli, S. Stagira, S. De Silvestri, and O. Svelto are with the Centro di Elettronica Quantistica e Strumentazione Elettronica-CNR, Dipartimento di Fisica, Politecnico, Istituto Nazionale per la Fisica della Materia, 20133 Milan, Italy.

S. Sartania, Z. Cheng, G. Tempea, Ch. Spielmann, and F. Krausz are with Abteilung Quantenelektronik und Lasertechnik Technische Universität Wien, A-1040 Vienna, Austria.

Publisher Item Identifier S 1077-260X(98)03841-6.

dispersion control over the above mentioned spectral range without the need for prisms. These mirrors have opened the way to scaling sub-10-fs hollow-fiber-based compressors to substantially higher pulse energies and hence, peak powers than previously possible. Recent experiments demonstrated the generation of 0.5-mJ 5-fs pulses at a repetition rate of 1 kHz [19]. Details about the design and characteristics of this novel ultrabroad-band mirrors are presented in a paper submitted to this same issue [20]. In this paper, we shall focus on the theoretical and experimental characterization of the hollow-fiber technique. The paper is organized as follows. Sections II and III are devoted to a theoretical analysis of the hollow fiber in term of mode characteristics and nonlinear pulse propagation, respectively. Spectral broadening and compression experiments with high-energy 20-fs pulses are presented in Section IV. Optimum conditions for pulse compression are outlined considering the role of SPM and gas dispersion. General design criteria to scale the compression technique toward the terawatt level are presented in Section V. Section VI briefly outlines a few applications of high-energy sub-10-fs pulses.

II. Hollow-Fiber Mode Characteristics

The use of the hollow fiber presents the advantages of a guiding element with a large-diameter single mode and of a fast nonlinear medium with a high threshold for multiphoton ionization. Wave propagation along hollow fibers can be thought of as occurring by grazing incidence reflections at the dielectric inner surface. Since the losses caused by these reflections greatly discriminate against higher order modes, only the fundamental mode, with large and scalable size, will be transmitted through a sufficiently long fiber. For fused silica gas-filled hollow fibers the fundamental mode is the EH_{11} hybrid mode, whose intensity profile as a function of the radial coordinate r is given by $I_0(r) = I_0 J_0^2(2.405r/a)$, where I_0 is the peak intensity, J_0 is the zero-order Bessel function and a is the capillary radius [21]. Since the field attenuation constant is proportional to λ^2/a^3, where λ is the laser wavelength, the losses can be made arbitrarily small by choosing a sufficiently large capillary radius. By proper mode matching, the incident radiation can be dominantly coupled into the fundamental propagation mode. Good mode coupling between the input beam and the excited hollow fiber mode is essential for proper operation of the compression stage. Mode-mismatch increases losses and introduces higher order modes excitation, lowering output beam quality and giving rise to intermodal dispersion. Considering propagation along the z-direction, the coupled power P_c can be approximately calculated, as in the case of optical fiber, using the following expression [22]: $P_c = \int\int \vec{E}_i \times \vec{H}_f \cdot \vec{e}_z \, dS$, where $\vec{E}_i$ is the electric field of the incident beam, $\vec{H}_f$ the magnetic field of the excited fiber mode, $\vec{e}_z$ the unity vector corresponding to the fiber axis z and dS the elementary fiber transverse section. This is an implicit relation, since the amplitude of $\vec{H}_f$ is unknown. Nevertheless, knowing the modal shapes of input and guided beams, it is possible to calculate the power transmission solving the previous integral. It is worth to point out that

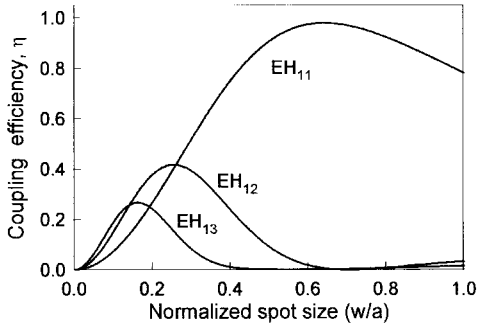

Fig. 1. Coupling efficiency η for the hollow fiber hybrid modes EH_{1m} (m = 1, 2, 3) as a function of the normalized input spot size w/a.

a linearly polarized input beam can only excite the EH_{1m} modes of the hollow fiber, which are the only ones showing a nonzero power coupling, since they are the only linearly polarized modes sustained by the hollow fiber. Assuming a Gaussian incident beam linearly polarized along the y-axis, with electric field $\vec{E}_i = E_0 \exp(-r^2/w^2)\vec{e}_y$, and the EH_{1m} hybrid modes, with magnetic field $\vec{H}_f = H_0 J_0(u_{1m} r/a)\vec{e}_x$, where u_{1m} is the mth root of the equation $J_0(u_{1m}) = 0$, it is possible to solve the equation for the coupled power. The coupling efficiency $\eta = P_c/P_{\text{in}}$, where P_{in} is the input power, turns out to be given by

$$\eta = \frac{4\left[\int r J_0(u_{1m} r/a) \exp(-r^2/w^2)\, dr\right]^2}{\left[w^2 \int r J_0^2(u_{1m} r/a)\, dr\right]}. \tag{1}$$

Fig. 1 shows the calculated coupling efficiency η of the EH_{1m} (m = 1, 2, 3) hybrid modes as a function of the input-beam spot size normalized to the capillary radius (w/a) in correspondence of the tip of the hollow fiber. From Fig. 1 the optimum value of w/a turns out to be 0.65. By proper mode-matching the coupling efficiency η for the fundamental EH_{11} mode is ~98%, while the corresponding η for the EH_{12} mode is ~0.5%. Note that to have a coupling efficiency larger than 90%, w/a can range from 0.49 to 0.84. For spot size values smaller than the optimum one the coupling efficiency for the fundamental mode drastically decreases and higher order modes are increasingly excited. In the optimum coupling condition mode discrimination of the fundamental mode from higher order modes is very high even with short hollow fibers.

Moreover, the hollow fiber preserves the polarization of the input radiation and, since it acts as a distributed spatial filter, suppressing high-frequency spatial components possibly present, output beam is expected to be diffraction limited. Profile measurements at different distances from the output of the fiber show indeed that the beam is virtually diffraction limited [17]–[19].

III. Nonlinear Pulse Propagation in a Gas-Filled Hollow Fiber

Pulse propagation in a gas-filled hollow fiber can be described by the same equations used for the case of optical fibers. Considering propagation along the z-direction, the

electric field for the fiber modes can be written as follows [23]:

$$E(\boldsymbol{r},\omega) = F(x,y)A(z,\omega)\exp[i\beta(\omega)z] \tag{2}$$

where $A(z,\omega)$ is the mode-amplitude, $F(x,y)$ is the mode-transverse-distribution and $\beta(\omega)$ is the mode-propagation constant. The propagation equation for the guided field splits in two equations for $A(z,\omega)$ and $F(x,y)$. In the first-order perturbation theory, a perturbation $\Delta n = \overline{n}_2|E|^2$ of the refractive index does not change the modal distribution $F(x,y)$, while the mode propagation constant $\overline{\beta}(\omega)$ can be written as $\overline{\beta}(\omega) = \beta(\omega) + \Delta\beta$, where the perturbation $\Delta\beta$ is given by

$$\Delta\beta = \frac{k_0 \int\int \Delta n|F(x,y)|^2\, dx\, dy}{\int\int |F(x,y)|^2\, dx\, dy} \tag{3}$$

where k_0 is the vacuum wave number. As it is evident from (3), the perturbation $\Delta\beta$, which includes the effect of fiber nonlinearity, is related to a spatial average on the fiber transverse section of the perturbation Δn. In this way, spatially uniform SPM and related spectral broadening can be realized.

After having performed the integration over the transverse coordinates, the treatment of nonlinear propagation reduces to a one-dimensional problem. Taking the inverse Fourier transform of the equation that describes the evolution of the mode amplitude A, it is possible to write the propagation equation for A in the time domain in a reference frame moving with the pulse at the group velocity v_g. Let us introduce a temporal scale normalized to the initial pulse half-width (at $1/e$-intensity point) T_0 through $\tau = (t - z/vg)/T_0$ and a normalized amplitude $U(z,\tau)$ using the definition:

$$A(z,\tau) = \sqrt{P_0}\exp(-\alpha z/2)U(z,\tau) \tag{4}$$

where P_0 is the peak power of the incident pulse and the exponential factor accounts for fiber losses. Assuming an instantaneous nonlinear response, the normalized amplitude U satisfies the following propagation equation [23]:

$$i\frac{\partial U}{\partial z} = \frac{\mathrm{sgn}(\beta_2)}{2L_d}\frac{\partial^2 U}{\partial \tau^2} + i\frac{\mathrm{sgn}(\beta_3)}{6L'_d}\frac{\partial^3 U}{\partial \tau^3} - \frac{e^{-\alpha z}}{L_{nl}} \cdot\left[|U|^2 U + \frac{i}{\omega_0 T_0}\frac{\partial}{\partial \tau}(|U|^2 U)\right] \tag{5}$$

where $\beta_2 = d^2\beta/d\omega^2$ is the GVD of the fiber, $\beta_3 = d^3\beta/d\omega^3$ is the third-order dispersion, $\mathrm{sgn}(\beta_i) = \pm 1$ $(i = 2, 3)$ depending on the sign of $\beta_i, L_d = T_0^2/|\beta_2|$ and $L'_d = T_0^3/|\beta_3|$ are the second- and third-order dispersion lengths, $L_{nl} = 1/\gamma P_0$ is the nonlinear length. The nonlinear coefficient γ is given by $\gamma = n_2\omega_0/cA_{\mathrm{eff}}$, where ω_0 is the center laser frequency, c is the speed of light in vacuum, n_2 is the nonlinear index coefficient ($n = n_0 + n_2 I$, where I is the field intensity) and A_{eff} is the effective mode area. The first term in the squared bracket of (5) describes the SPM-process, the second one governs the self-steepening effect, which leads to an asymmetry in the SPM-broadened spectra. The dispersion lengths L_d, L'_d and the nonlinear length L_{nl} give the length scales over which the dispersive or nonlinear effects become important for pulse evolution along the fiber. Optimum exploitation of the interplay between GVD and SPM for the generation of linearly chirped pulses calls for an optimum propagation length $L_{\mathrm{opt}} \approx (6L_{nl}L_d)^{1/2}$ [24], which shows the relative importance of both the GVD and SPM effects for good pulse compression.

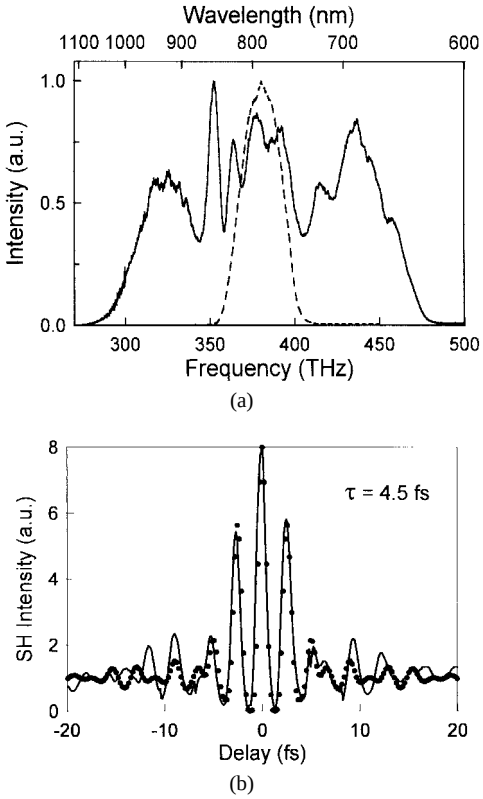

Fig. 2. (a) Spectral broadening in krypton at $p = 2.1$ bar and $P_0 = 2$ GW. The spectrum of the input pulses is shown as dashed line. (b) Measured (solid line) and calculated (dots) interferometric autocorrelation trace of the compressed pulses; an evaluation of the pulse duration (FWHM) is also given.

IV. Spectral Broadening and Pulse Compression

Previous experiments were performed using 20-fs input pulses with an energy of 40 μJ, and a 60-cm-long hollow fiber with an inner radius of 80 μm filled with krypton. A typical broadened spectrum for a krypton pressure $p = 2.1$ bar is shown in Fig. 2(a). Assuming for krypton $\eta_2 = n_2/p = 2.78 \times 10^{-23}$ m^2/W bar [25] and $\beta_2 \approx 60$ fs^2/m [21], [26] one obtains $L_{nl} \approx 1.1$ cm, $L_d \approx 2$ m. These values provide $L_{\mathrm{opt}} \approx 36$ cm, which is close to that used in the experiments. The frequency broadened pulses emerging from the hollow fiber were collimated and propagated through a dispersive delay line based on chirped mirrors and two pairs of fused silica prisms of small apex angle (20°). Fig. 2(b) shows the measured interferometric second harmonic autocorrelation trace of the compressed pulse. From this trace, a pulse duration of 4.5 fs (FWHM) was evaluated. Pulse energy after compression was 20 μJ [17], [18].

Scaling the input energy to higher values we demonstrated the generation of sub-10-fs pulses at the subterawatt peak power level [19]. Details on the experimental set-up are given in [19]. 20-fs input pulses with an energy of 1 mJ were coupled

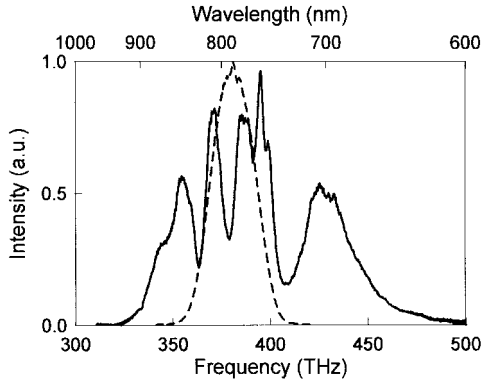

(a)

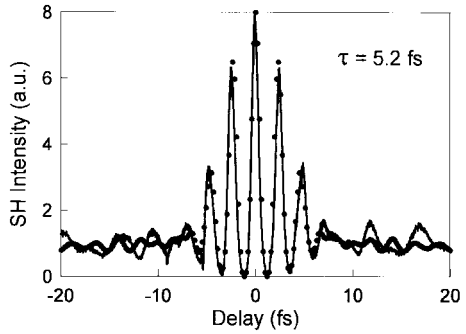

(b)

Fig. 3. (a) Spectral broadening in argon at $p = 0.5$ bar and $P_0 = 50$ GW. The spectrum of the input pulses is shown as dashed line. (b) Measured (solid line) and calculated (dots) interferometric autocorrelation trace of the compressed pulses; an evaluation of the pulse duration (FWHM) is also given.

into a 85-cm-long hollow fiber with an inner radius of 130 μm, filled with argon. A typical broadened spectrum for an argon pressure $p = 0.5$ bar is shown in Fig. 3(a). Assuming for argon $\eta_2 = 9.8 \times 10^{-24}$ m^2/W bar [25] and $\beta_2 \approx 2.8$ fs^2/m [21], [26], one obtains $L_{nl} \approx 1.3$ cm and $L_d \approx 45$ m, so that the optimum length turns out to be $L_{\rm opt} \approx 1.8$ m, which is 2.2 times larger than that used in the experiments. This is due to the fact that the effect of dispersion is less pronounced with respect to the previous case, as it is also evident from the spectrum of Fig. 3(a), which presents a deeper modulation. After recollimation by a silver mirror the beam is directed toward the dispersive delay line. At the millijoule level the prism-chirped-mirror compressor previously described cannot be employed because of self-focusing in the prisms. In this case, only ultrabroad-band chirped dielectric mirrors were used. Owing to a novel design technique [20], these chirped mirrors introduce a nearly constant negative group-delay dispersion over a spectral range as broad as 150 THz (650–950 nm), and exhibit a high reflectivity over the wavelength range of 600–1000 nm. The overall transmissivity of the compressor, including the recollimating and steering optics, is ≈80%. The compressed pulses were measured by interferometric second-harmonic autocorrelation. The second-order interferometric autocorrelation signal is generated in a 15-μm-thick BBO frequency doubling crystal and recorded at a scan rate of 1 Hz. To evaluate the pulse duration, we took the inverse Fourier transform of the spectrum and assumed, as free parameter, some residual cubic phase distortion, $(d^3\phi/d\omega^3)$.

TABLE I
MAXIMUM PEAK INTENSITY $I_{\max}$ IONIZATION DEGREE N, REFRACTIVE INDEX CHANGES DUE TO PLASMA (Δn_p) AND TO KERR EFFECT $(n_2 \cdot I_{\max})$, AND THEIR RATIO, FOR THREE DIFFERENT PULSE DURATIONS τ_0

τ_0 (fs)	I_{max} ($\times 10^{14}$ W/cm^2)	N ($\times 10^{-5}$)	Δn_p ($\times 10^{-7}$ bar^{-1})	$n_2 \cdot I_{max}$ ($\times 10^{-6}$ bar^{-1})	$n_2 \cdot I_{max}/\Delta n_p$
20	2.018	3.49	2.638	1.493	5.66
50	1.807	3.15	2.381	1.337	5.61
125	1.635	2.98	2.253	1.210	5.36

By best compression of the pulse whose spectrum is shown in Fig. 3(a), we measured the interferometric autocorrelation trace of Fig. 3(b). From this trace a pulse duration of 5.2 fs (FWHM) was evaluated. In the absence of spectral phase modulation we obtain a Fourier-transformed pulse width of 4.9 fs, indicating that the generated pulses are almost transform limited. Pulse energy after compression was 0.5 mJ, which corresponds to a peak intensity of 0.1 TW. Since the output beam is almost diffraction limited, it is expected to be focusable to irradiances in excess of 10^{17} W/cm^2.

V. TOWARDS SUB-10-fs PULSES WITH TERAWATT PEAK POWER

The potential scalability of this compression technique to higher pulse energies is an important issue considering the current availability of 20-fs laser pulses with peak powers up to the terawatt level. The laser peak power must be smaller than the critical power $P_{\rm cr}$ for self-focusing (for a Gaussian beam $P_{\rm cr} = \lambda^2/2\pi n_2$), which is determined by the type of gas used and by its pressure. Moreover, the maximum laser peak intensity is determined by the threshold for tunnel ionization. This represents a constraint to the hollow fiber diameter and to the type of gas. For pulse energy in the range of a few millijoules neon or helium seem to be the best choices. We first calculated the maximum pulse peak intensity for which the refractive index variation due to the Kerr effect $(\Delta n = n_2 I)$ dominates, by a factor of ∼5, the plasma nonlinearity $(\Delta n_p = \omega_p^2/2\omega_0^2$, where ω_p is the plasma frequency). The calculated maximum intensities $I_{\max}$ are reported in Table I for three pulse durations, together with the degree of ionization $N = n_{\rm ionized}/n_{\rm neutral}$, the changes in refractive index due to plasma Δn_p (normalized to the pressure) and to Kerr effect $\Delta n = \eta_2 I_{\max}$, and the ratio $\Delta n/\Delta n_p$. For determining the ion density we have considered only the tunnel ionization, which should be the dominant process. This maximum intensity, together with the input peak power P_0, determines the minimum capillary effective area $A_{\rm eff,min} = P_0/I_{\max}$. Since the maximum input peak power is determined by the critical power $P_{\rm cr}$, the maximum usable gas pressure turns out to be given by $p_{\max} = \lambda^2/2\pi\eta_2 P_0$. Fiber length l can be evaluated considering the following expression for the spectral broadening $\Delta\omega$, valid for Gaussian input pulses in the absence of dispersion [23]:

$$\Delta\omega = 2.86\gamma P_0 z_{\rm eff}/\tau_0 \tag{6}$$

where τ_0 is the input pulse duration (FWHM), and $z_{\rm eff}$ is

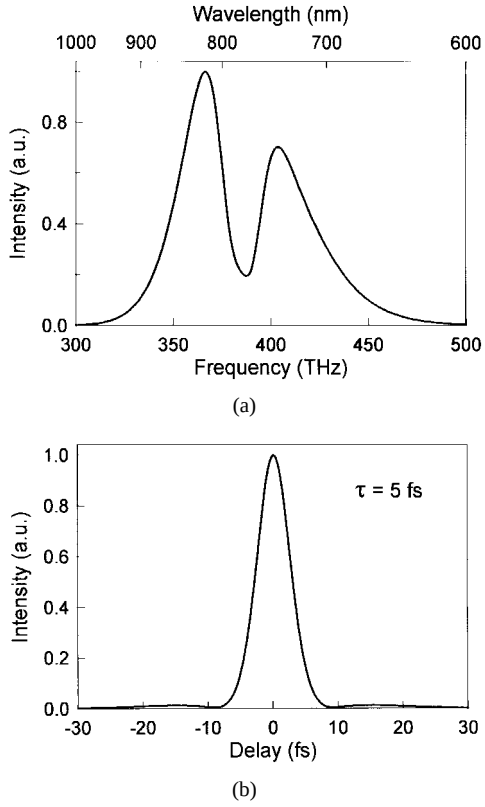

Fig. 4. (a) Spectral broadening obtained by computer simulations of the propagation of 20-fs 4-mJ pulses along a 50-cm-long 258-μm inner radius hollow fiber filled with neon at $p = 0.65$ bar. (b) Intensity profile of the ideally compressed pulse.

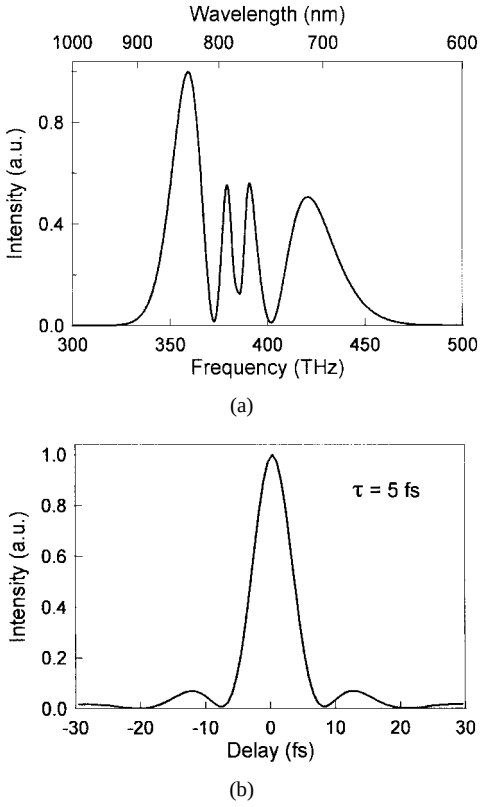

Fig. 5. (a) Spectral broadening obtained by computer simulations of the propagation of 50-fs 4-mJ pulses along a 55-cm-long 172-μm inner radius hollow fiber filled with neon at $p = 1.64$ bar. (b) Intensity profile of the ideally compressed pulse.

TABLE II
FIBER PARAMETERS (RADIUS a, MINIMUM LENGTH $l_{\min}$ AND MAXIMUM GAS PRESSURE $p_{\max}$) OBTAINED FROM THE DESIGN PROCEDURE DESCRIBED IN THE TEXT, FOR INPUT PULSE WITH THE SAME ENERGY E AND DIFFERENT DURATIONS τ_0

τ_0 (fs)	E (mJ)	a (μm)	l_{min} (cm)	p_{max} (bar)
20	4	258	50	0.65
50	4	172	55	1.64
125	4	114	61	4.1

the effective propagation length, which, in the case of large aperture fiber, can be assumed to be equal to l. Assuming an ideally compressed pulse with duration τ_c (FWHM) and Gaussian spectrum, the corresponding spectral width is given by $\Delta\omega = 1.664/\tau_c$. Therefore, the minimum fiber length turns out to be given by

$$l_{\min} = 0.154 \frac{\tau_0}{\tau_c} \frac{\lambda}{\eta_2 p_{\max} I_{\max}}. \tag{7}$$

Note that the numerical factor in (7) depends on the actual shape of the broadened spectrum.

Using the previous general design criteria, we have performed computer simulations of the nonlinear propagation of high energy pulses with different duration (20, 50, and 125 fs) in hollow fibers filled with neon. The simulations were performed applying the split-step Fourier method to the nonlinear propagation equation (5). In the case of 20-fs, 4-mJ input pulses, using the $I_{\max}$ value reported in Table I, we obtain $A_{\text{eff,min}} = 9.9 \times 10^{-8}$ m^2, which corresponds to a capillary radius $a = 258$ μm. Assuming for neon $\eta_2 = 7.4 \times 10^{-25}$ m^2/W bar [25] the maximum pressure turns out to be $p_{\max} = 0.65$ bar. In order to obtain a spectral broadening Δw suitable to sustain a pulse with duration $\tau_c = 5$ fs, the minimum fiber length, using (7), is given by $l_{\min} = 50$ cm. Fig. 4(a) shows the calculated spectral broadening obtained using the previously calculated parameters. Simple estimation of the losses due to plasma generation yields that they can be neglected for the parameter regime in consideration [27]. It is worth to note that no further parameter adjustment is needed to achieve the desired spectral width. This indicates that in this case (6) gives a good estimation of the spectral broadening since the dispersion is almost negligible ($|\beta_2| \approx 0.5$ fs^2/m [21], [26]). The compressed pulse, whose intensity profile assuming a perfect dispersion compensation is shown in Fig. 4(b), has relatively small wings. Calculated pulse duration is 5 fs. Assuming an overall transmission, including hollow fiber and compressor, of ≈70%, this corresponds to a peak intensity of 0.56 TW. It is worth to note that, even if the actual η_2 value can be different from the quoted one, in order to obtain the same n_2 value one has simply to rescale gas pressure.

In the case of 50- and 125-fs, 4-mJ input pulses, using the $I_{\max}$ values reported in Table I, we obtained the fiber parameters reported in Table II. Fig. 5(a)–(b) shows the corresponding spectral broadening and intensity profile of the

ideally compressed pulse, obtained by computer simulation for 50-fs input pulses. The spectrum presents deep amplitude modulations typical of a pure SPM-process; consequently the compressed pulse shows more pronounced wings.

VI. Applications

The generation of diffraction-limited multigigawatt light pulses in the single-cycle regime promises to be a powerful tool for precisely triggering and controlling the evolution of atomic systems in strong laser fields. Many applications will benefit from this capability in the future. Perhaps one of the most challenging one is the generation and control of high-order harmonic radiation in the soft X-ray spectral region. Coherent X-ray are significant for a number of fields in science and technology because of their potential for providing high spatial and temporal resolution. Intense, spatially coherent laser-generated X-rays in the "water-window" (2.33–4.36 nm) will make significant impacts on high-resolution X-ray microscopy and holography of living cell in biology [28]. Since the duration of these X-ray pulses is expected to be shorter than that of the exciting light pulse, their use for time-resolved X-ray diffraction will allow studying chemical reactions and structural changes of condensed matter with never-before-achieved time resolution. Coherent extreme ultraviolet radiation extending into the water window has been generated at a repetition rate of 1 kHz by focusing 5-fs 0.1-TW pulses in a helium gas jet [29]. The incident light field contains just a few oscillations, which results in the emission of a X-ray super continuum. Owing to the extremely short rise time of the driving pulses neutral atoms can be exposed to very high fields before ionization. As a result, the observed spatially coherent X-ray continuum extends to wavelength as short as 2.4 nm (photon energy: 0.5 keV) and is delivered in a well-collimated beam. This compact system holds promise as a laboratory-scale source for biological holography and nonlinear optics in the X-ray regime.

Acknowledgment

The authors wish to thank K. Ferencz from the Research Institute for Solid State Physics Budapest for the design and manufacturing of the chirped mirrors.

References

[1] R. L. Fork, B. I. Green, and C. V. Shank, "Generation of optical pulses shorter than 0.1 ps by colliding pulse mode locking," *Appl. Phys. Lett.*, vol. 38, pp. 671–672, 1981.

[2] J. A. Valdmanis, R. L. Fork, and J. P. Gordon, "Generation of optical pulses as short as 27 femtoseconds directly from a laser balancing self-phase modulation, group-velocity dispersion, saturable absorption, and saturable gain," *Opt. Lett.*, vol. 10, pp. 131–133, 1985.

[3] D. E. Spence, P. N. Kean, and W. Sibbett, "60-fs pulse generation from a self-mode-locked Ti:sapphire laser," *Opt. Lett.*, vol. 16, pp. 42–44, 1991.

[4] L. Xu, Ch. Spielmann, F. Krausz, and R. Szipöcs, "Ultrabroad ring oscillator for sub-10-fs pulse generation," *Opt. Lett.*, vol. 21, pp. 1259–1261, 1996.

[5] I. D. Jung, F. X. Kärtner, N. Matuschek, D. H. Sutter, F. Morier-Genoud, G. Zhang, U. Keller, V. Scheuer, M. Tilsch, and T. Tschudi, "Self-starting 6.5-fs pulses from a Ti:sapphire laser," *Opt. Lett.*, vol. 22, pp. 1009–1011, 1997.

[6] D. Strickland and G. Mourou, "Compression of amplified chirped optical pulses," *Opt. Commun.*, vol. 56, pp. 219–221, 1985.

[7] J. Zhou, C. P. Huang, M. M. Murnane, and H. C. Kapteyn, "Amplification of 26-fs, 2-TW pulses near the gain-narrowing limit in Ti:sapphire," *Opt. Lett.*, vol. 20, pp. 64–66, 1995.

[8] C. P. J. Barty, T. Guo, C. Le Blanc, F. Raksi, C. R.-P. Petruck, J. Squier, K. R. Wilson, V. V. Yakovlev, and K. Yamakawa, "Generation of 18-fs, multiterawatt pulses by regenerative pulse shaping and chirped-pulse amplification," *Opt. Lett.*, vol. 21, pp. 668–670, 1996.

[9] J. P. Chambaret, C. Le Blanc, G. Chériaux, P. Curley, G. Darpentigny, P. Rousseau, G. Hamoniaux, A. Antonetti, and F. Salin, "Generation of 25-TW, 32-fs pulses at 10 Hz," *Opt. Lett.*, vol. 21, pp. 1921–1923, 1996.

[10] M. Lenzner, Ch. Spielmann, E. Wintner, F. Krausz, and A. J. Schmidt, "Sub-20-fs, kilohertz-repetition-rate Ti:sapphire amplifier," *Opt. Lett.*, vol. 20, pp. 1397–1399, 1995.

[11] S. Backus, J. Peatross, C. P. Huang, M. M. Murnane, and H. C. Kapteyn, "Ti:sapphire amplifier producing millijoule-level 21-fs pulses at 1 kHz," *Opt. Lett.*, vol. 20, pp. 2000–2002, 1995.

[12] H. Nakatsuka, D. Grischkowsky, and A. C. Balant, "Nonlinear picosecond-pulse propagation through optical fibers with positive group velocity dispersion," *Phys. Rev. Lett.*, vol. 47, pp. 910–913, 1981.

[13] R. L. Fork, C. H. Brito Cruz, P. Becker, and C. V. Shank, "Compression of optical pulses to six femtoseconds by using cubic phase compensation," *Opt. Lett.*, vol. 12, pp. 483–485, 1987.

[14] A. Baltuska, Z. Wei, M. S. Pshenichnikov, and D. A. Wiersma, "Optical pulse compression to 5 fs at a 1-MHz repetition rate," *Opt. Lett.*, vol. 22, pp. 102–104, 1997.

[15] A. Baltuska, Z. Wei, R. Szipöcs, M. S. Pshenichnikov, and D. A. Wiersma, "All solid-state cavity-dumped sub-5-fs laser," *Appl. Phys. B*, vol. 65, pp. 175–188, 1997.

[16] M. Nisoli, S. De Silvestri, and O. Svelto, "Generation of high energy 10-fs pulses by a new pulse compression technique," *Appl. Phys. Lett.*, vol. 68, pp. 2793–2795, 1996.

[17] M. Nisoli, S. De Silvestri, O. Svelto, R. Szipöcs, K. Ferencz, Ch. Spielmann, S. Sartania, and F. Krausz, "Compression of high-energy laser pulses below 5 fs," *Opt. Lett.*, vol. 22, pp. 522–524, 1997.

[18] M. Nisoli, S. Stagira, S. De Silvestri, O. Svelto, S. Sartania, Z. Cheng, M. Lenzner, Ch. Spielmann, and F. Krausz, "A novel high energy pulse compression system: Generation of multigigawatt sub-5-fs pulses," *Appl. Phys. B*, vol. 65, pp. 189–196, 1997.

[19] S. Sartania, Z. Cheng, M. Lenzner, G. Tempea, Ch. Spielmann, F. Krausz, and K. Ferencz, "Generation of 0.1-TW 5-fs optical pulses at a 1-kHz repetition rate," *Opt. Lett.*, vol. 22, pp. 1526–1528, 1997.

[20] G. Tempea, F. Krausz, Ch. Spielmann, and K. Ferencz, "Dispersion control over 150 THz with chirped dielectric mirrors," this issue, pp. 193–196.

[21] E. A. J. Marcatili and R. A. Schmeltzer, "Hollow metallic and dielectric waveguides for long distance optical transmission and lasers," *Bell Syst. Tech. J.*, vol. 43, pp. 1783–1809, 1964.

[22] E.-G. Neumann, *Single-Mode Fibers*. Berlin, Germany: Springer-Verlag, 1988.

[23] G. P. Agrawal, *Nonlinear Fiber Optics*. San Diego, CA: Academic, 1995.

[24] W. J. Tomlinson, R. H. Stolen, and C. V. Shank, "Compression of optical pulses chirped by self-phase modulation in fibers," *J. Opt. Soc. Amer. B*, vol. 1, pp. 139–149, 1984.

[25] H. J. Lehmeier, W. Leupacher, and A. Penzkofer, "Nonresonant third order hyperpolarizability of rare gases and N_2 determined by third harmonic generation," *Opt. Commun.*, vol. 56, pp. 67–72, 1985.

[26] A. Dalgarno and A. E. Kingston, "The refractive indices and Verdet constants of the inert gases," *Proc. R. Soc. Lon. A*, vol. 259, pp. 424–429, 1966.

[27] T. Brabec and G. Tempea, private communication.

[28] H. B. Stuhrmann, Ed., *Uses of Synchrotron Radiation in Biology*. New York: Academic, 1982.

[29] Ch. Spielmann, N. H. Burnett, S. Sartania, R. Koppitsch, M. Schnurer, C. Kan, M. Lenzner, P. Wobrauschek, and F. Krausz, *Science*, vol. 278, pp. 661–664.

M. Nisoli, photograph and biography not available at the time of publication.

S. Stagira, photograph and biography not available at the time of publication.

S. De Silvestri, photograph and biography not available at the time of publication.

O. Svelto, photograph and biography not available at the time of publication.

S. Sartania, photograph and biography not available at the time of publication.

Z. Cheng, photograph and biography not available at the time of publication.

Gabriel Tempea, for photograph and biography, see this issue, p. 196.

Christian Spielmann, for photograph and biography, see this issue, p. 184.

Ferenc Krausz (M'92), for photograph and biography, see this issue, p. 184.